American Welding Society®

For rapid publication of innovative, leading-edge research on joining and additive manufacturing topics in the *Welding Journal Research Supplement*

WJRS LETTERS

Wire-Based Friction Stir Additive Manufacturing toward Field Repairing

A new process is introduced for repair of structural components of aluminum alloys

BY H. CHEN, J. CHEN, S. XU, Y. ZHAO, X. MENG, Y. XIE, AND Y. HUANG

■ **Keywords:** Additive manufacturing, maintenance and repair welding, Al alloy, mechanical properties

Introduction

Lightweight alloy parts often experience substantial wear, corrosion, or chemical reactions in service, resulting in significant areal and volumetric defects (Refs. 1, 2). Replacement of these worn out parts is often economically impractical and leads to the waste of resources. In recent years, continuous efforts have been taken to extend the service life of worn out lightweight alloy parts with reliable field repair regimes (Ref. 3). Field repair, which is aimed at restoring the part's original geometry and improving its mechanical performance, can reduce the costs dramatically. Conventional fusion-based repair technologies are accompanied by inherent issues with solidification defects, such as grain coarsening, porosity, and cracks, resulting in repaired parts with poor performance (Refs. 4, 5). It is desirable to devise a solid-state repair technology that can impart low thermoinduced softening (Refs. 6–8) to avoid melting and solidification defects and to realize high-quality repair of volumetric defects. The major benefits of friction-based additive manufacturing involve the ability to fabricate aluminum parts that are free from thermal damage and porosity (Ref. 9). Several related friction-based additive manufacturing technologies have been developed, including friction surfacing and additive friction stir deposition (Refs. 10, 11). The noncontinuous procedure for feeding materials in these friction-based additive manufacturing processes led to an unstable processing and performance in field repairs (Ref. 12).

The present study is aimed at issues related to large cracks or partial wear in aluminum alloy structural parts. A solid-state repair approach, named wire-based friction stir additive manufacturing (W-FSAM), was proposed. It can enable continuous feeding wire without large axial force compared to conventional solid-state repair technologies and is suitable for field repairs. The benefits of W-FSAM in field repairs are evaluated by the design strategy of the components and interfacial microstructures and properties.

Experimental Procedures

A schematic of the solid-state repair technique W-FSAM is shown in Fig. 1. Components included a storage chamber with a wire feeding hole and a pin with a screw feature, and three probes were produced from H13 steel. The diameter of the movable shoulder at the root of the probes was 14 mm, and the diameter of the stationary shoulder on the storage chamber was 24 mm. These features were used to forge the filler materials. The three probes on the bottom surface of the pin were designed to stir the filler materials. A groove on the sheet surface was premachined with 8 mm in width and 1 mm in depth. In the W-FSAM process, the screw topology was utilized to continuously thermoplasticize feeding wire and squeeze the materials downward through severe plastic deformation (SPD) and corresponding frictional heat. A wire feed speed of 3000 mm/min, rotational velocity of 1200 rpm, advancing speed of 600 mm/min, and a plunge depth of 0.1 mm below the bottom of the groove for the probes were selected. The base metal (BM) was an AA6061-T4 sheet with a thickness of 6 mm. The feedstock materials were Al-Si (Al-5%Si) alloy wires 2.4 mm in diameter.

The optical microscopy (OM, VHX-1000E) specimen was etched with an 8% hydrofluoric acid aqueous solution to reveal the microstructures. Microhardness mapping was measured at a load of 100 g with a dwell time of 10 s using an HXD-1000TM Vickers tester. Flat tensile specimens with dimensions of 110 mm in length, 12.5 mm in width, and 6 mm in thickness were employed. Tensile properties were assessed with a crosshead rate of 2 mm/min by a Shimadzu

https://doi.org/10.29391/2022.101.019

AG-Xplus testing machine. The fracture morphologies of tensile specimens were observed by using a scanning electron microscope (Merlin Compact).

Results and Discussion

The characterization results of the W-FSAM joint are shown in Fig. 2. The geometry of the groove is depicted in Fig. 2A. In the W-FSAM process, the threaded pin can convey and squeeze the thermoplasticized materials continuously. The probes of the pin facilitate the plastic flow of filling materials within the prerepair groove. A top view of the repaired component is shown in Fig. 2C, and a side view of the repair can be seen in Fig. 2B. The repaired grooves filled by the Al-Si alloy via W-FSAM were well-bonded. The microhardness of the repaired zone was 55.8 ± 5.8 HV, which reached 92% of the base metal — Fig. 2D. Microhardness values on the advancing side (AS) were lower than on the retreating side (RS) within the repaired zone. The microhardness around the bonding interfaces between the filler materials and the groove was higher than the interior of the repaired zone. Thermomechanically affected zones formed by the shear forces at the bonding interfaces. During the repair process, the thermoplasticized materials could directly contact boundaries of the groove with the stirring effect of probes. This promoted heat loss, causing fine grains.

Higher magnification views of regions of Fig. 2B are provided in Figs. 3A–D. During the W-FSAM process, grains in the repaired zone experienced sufficient dynamic recrystallization induced by SPD and were further refined — Fig. 3. SPD is mainly caused by the combination of frictional heat and high strain rates. The bonding interfaces between the filler materials and the groove are revealed in Figs. 3B–D. The stirring effects of the probes had a significant influence on the formation of the repaired joint. There was an indistinct and wavy interface bonding at the bottom of the repaired groove, which showed a good metallurgical bond. The frictional heat of rotational probes was beneficial to increasing the material flow behavior. Figures 3C and D show the bonding interfaces between the repaired zone and side boundaries of the groove at the advancing side and retreating side. Interestingly, during the repair process, the basel metal around the original sides of the groove and filler materials were plasticized by a thermomechanical coupled effect of components. SPD promoted dynamic recrystallization around the original boundaries of

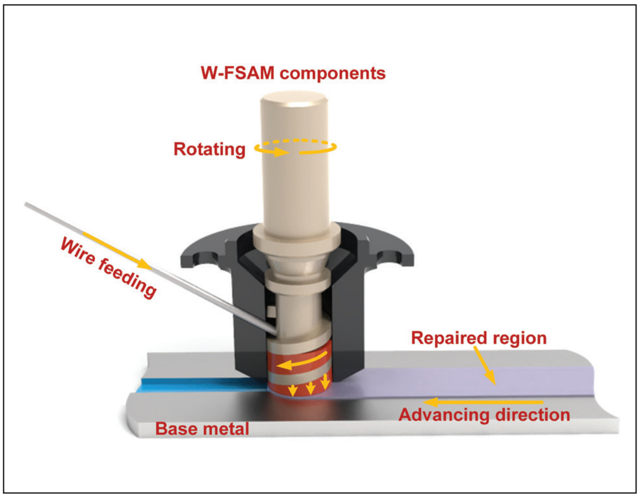

Fig. 1 — Schematic of the W-FSAM technique.

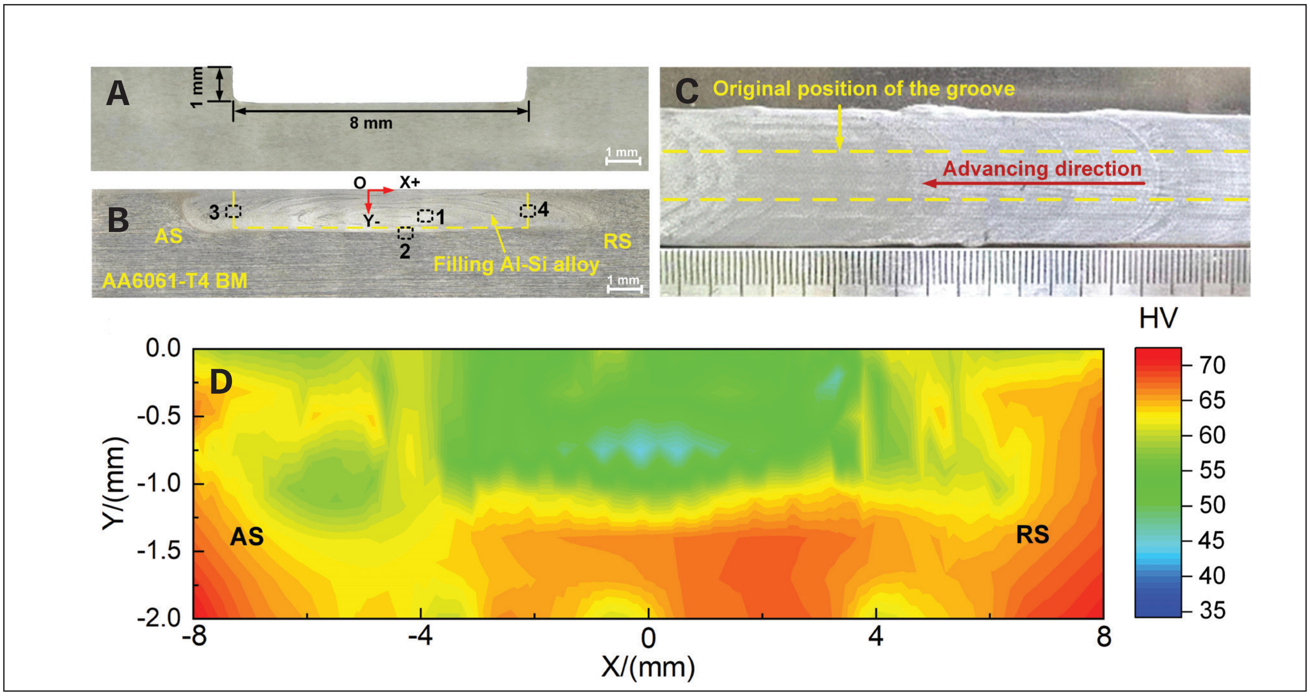

Fig. 2 — Characterization of the W-FSAM joint: A — Geometry of the groove; B — cross-sectional image of the repaired joint; C — the repaired joint with the featured marks; D — microhardness mapping.

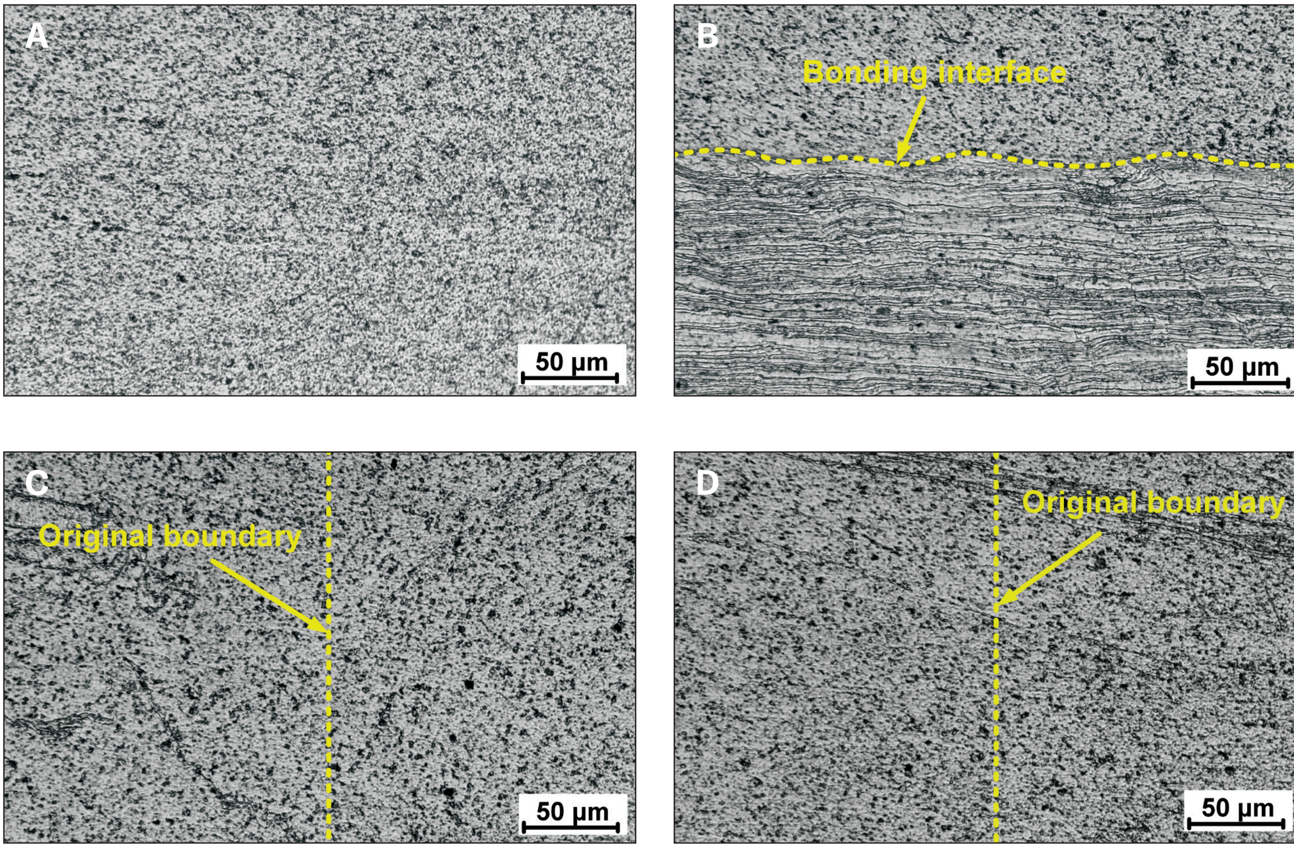

Fig. 3 — Microstructures: A — Repaired zone; B — bonding interface at the bottom of the groove; and bonding interfaces between the repaired zone and side boundaries at C — AS; D — RS.

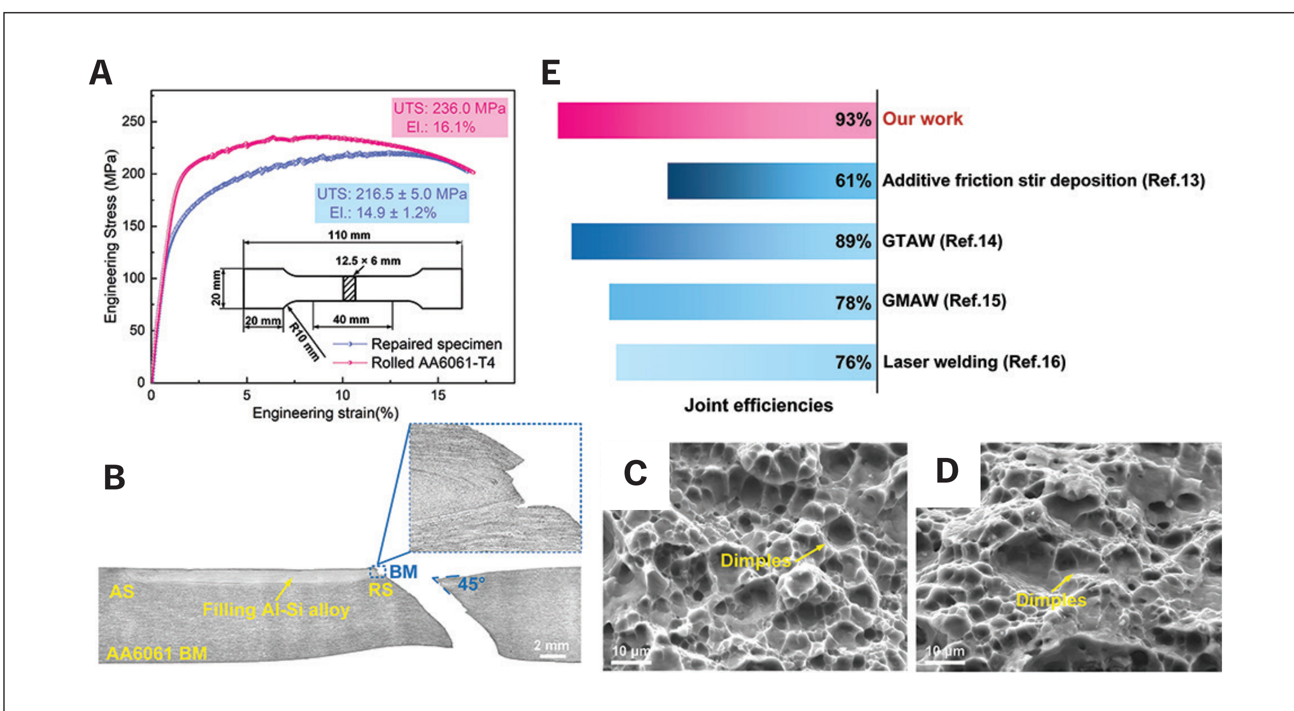

Fig. 4 — The tensile properties of repaired specimens: A — Engineering stress-strain curves by W-FSAM vs. BM; B — the fracture location of the typical tensile specimen; fracture morphologies in C — repairing region and D — BM; E — joint efficiencies by different repairing methods (Refs. 13–16).

the groove, and the fine recrystallized grains were formed within these areas.

Engineering stress vs. strain curves of rolled AA6061-T4 base metal and repaired specimens with ultimate tensile strength (UTS) and elongation are depicted in Fig. 4A. The measured UTS and elongation of the repaired specimens were 216.5 ± 5.0 MPa and 14.9 ± 1.2%, which reached 93 and 98% of the base metal in terms of UTS and percent elongation, respectively. The fracture locations of the tensile specimen are shown in Fig. 4B. The upper fracture location was near the boundary between the repaired zone and the base metal on the retreating side. This area is associated with the relatively weak zone induced by the thermomechanical effect on the deformation of microstructures. Figures 4C and D present the fracture morphologies of the repaired zone and base metal. There were many shallow dimples in the fracture morphologies of the repaired zone and base metal, indicating ductile fracture. The joint efficiency was compared to the other repairing technologies, as shown in Fig. 4E. Our process can reach 93% of the base metal in terms of UTS. This percentage is higher than other weld repair technologies. The W-FSAM repair strategy can achieve the quasi-equal-strength repairing of aluminum alloy.

Conclusion

A W-FSAM technique was proposed to repair the volumetric defects in structural parts. The screw topology conveyed the thermoplasticized materials continuously, and the probes promoted effective bonding of the filler materials and boundaries of the groove. The W-FSAM technique enabled sufficient bonding and filling between the feeding materials and side boundaries of the groove, and the repaired zone exhibited recrystallized grains. The W-FSAM repair approach achieved tensile properties of repaired parts reaching 93 and 98% of the base metal in terms of UTS and percent elongation, respectively. Our work expands the design latitude toward field repair and provides opportunities to explore quasi-equal-strength repair applications.

Acknowledgments

This work was greatly supported by the National Natural Science Foundation of China (No. 52175301), the China National Postdoctoral Program for Innovative Talents (No. BX20220384), and the Shanghai Aerospace Science and Technology Innovation Fund of China (No. SAST2020-108).

References

1. Meng, X., Huang, Y., Cao, J., Shen, J., and dos Santos, J. F. 2021. Recent progress on control strategies for inherent issues in friction stir welding. *Progress in Materials Science* 115: 100706. DOI: 10.1016/j.pmatsci.2020.100706

2. Gottwald, R. B., Griffiths, R. J., Petersen, D. T., Perry, M. E. J., and Yu, H. Z. 2021. Solid-state metal additive manufacturing for structural repair. *Accounts of Materials Research* 2(9): 780–792. DOI: 10.1021/accountsmr.1c00098

3. Chen, K., Huang, R., Li, Y., Lin, S., Zhu, W., Tamura, N., Li, J., Shan, Z., and Ma, E. 2020. Rafting-enabled recovery avoids recrystallization in 3D-printing-repaired single-crystal superalloys. *Advanced Materials* 32(12): 1907164. DOI: 10.1002/adma.201907164

4. Vishnukumar, M., Pramod, R., and Rajesh Kannan, A. 2021. Wire arc additive manufacturing for repairing aluminium structures in marine applications. *Materials Letter* 299: 130112. DOI: 10.1016/j.matlet.2021.130112

5. Eff, M., Hack, H., Shipley, D., and Shira, S. 2022. The effects of postweld processing on friction stir welded, additive manufactured AlSi10Mg. *Welding Journal* 101(4): 111-s to 122-s. DOI: 10.29391/2022.101.009

6. Liu, X., and Sun, Z. 2022. Numerical simulation of vortex-friction stir welding based on internal friction between identical materials. *International Journal of Heat and Mass Transfer* 185: 122418. DOI: 10.1016/j.ijheatmasstransfer.2021.122418

7. Xie, Y., Meng, X., and Huang, Y. 2022. Entire process simulation of friction stir welding — Part 1: Experiments and simulation. *Welding Journal* 101(5): 144–159. DOI: 10.29391/2022.101.011

8. Xie, Y., Meng, X., Chang, Y., Mao, D., Qin, Z., Wan, L., and Huang, Y. 2022. Heteroatom modification enhances corrosion durability in high-mechanical-performance graphene-reinforced aluminum matrix composites. *Advanced Science* 2104464: 1–9. DOI: 10.1002/advs.202104464

9. Mason, C. J. T., Rodriguez, R. I., Avery, D. Z., Phillips, B. J., Bernarding, B. P., Williams, M. B., Cobbs, S. D., Jordon, J. B., and Allison, P. G. 2021. Process-structure-property relations for as-deposited solid-state additively manufactured high-strength aluminum alloy. *Additive Manufacturing* 40: 101879. DOI: 10.1016/j.addma.2021.101879

10. Khodabakhshi, F., and Gerlich, A. P. 2018. Potentials and strategies of solid-state additive friction-stir manufacturing technology: A critical review. *Journal of Manufacturing Processes* 36: 77–92. DOI: 10.1016/j.jmapro.2018.09.030

11. Damodaram, R., Rai, P., Cyril Joseph Daniel, S., Bauri, R., and Yadav, D. 2021. Friction surfacing: A tool for surface crack repair. *Surface and Coatings Technology* 422: 127482. DOI: 10.1016/j.surfcoat.2021.127482

12. Ward, A. A., and Cordero, Z. C. 2020. Junction growth and interdiffusion during ultrasonic additive manufacturing of multi-material laminates. *Scripta Materialia* 177: 101–105. DOI: 10.1016/j.scriptamat.2019.10.004

13. Martin, L. P., Luccitti, A., and Walluk, M. 2022. Repair of aluminum 6061 plate by additive friction stir deposition. *International Journal of Advanced Manufacturing Technology* 118(3–4): 759–773. DOI: 10.1007/s00170-021-07953-z

14. Maya-Johnson, S., Santa, J. F., Mejía, O. L., Aristizábal, S., Ospina, S., Cortés, P. A., and Giraldo, J. E. 2015. Effect of the number of welding repairs with GTAW on the mechanical behavior of AA7020 aluminum alloy welded joints. *Metallurgical and Materials Transactions B* 46(5): 2332–2339. DOI: 10.1007/s11663-015-0416-9

15. Li, S., Dong, H., Wang, X., Liu, Z., Tan, Z., Shangguan, L., Lu, Q., and Zhong, S. 2020. Effect of repair welding on microstructure and mechanical properties of 7N01 aluminum alloy MIG welded joint. *Journal of Manufacturing Processes* 54: 80–88. DOI: 10.1016/j.jmapro.2020.03.009

16. Tu, J., and Paleocrassas, A. 2010. Low speed laser welding of aluminum alloys using single-mode fiber lasers. In *Laser Welding*, edited by Na, X., 47–77. London, U.K.: InTechOpen Ltd. DOI: 10.5772/9857

HUIZI CHEN, JIALIN CHEN, XIANGCHEN MENG, YUMING XIE, and **YONGXIAN HUANG** (*yxhuang@hit.edu.cn*) are with the State Key Laboratory of Advanced Welding and Joining, Harbin Institute of Technology, Harbin, China. **SHUANGMING XU** is with the China Aerospace Science and Technology Corp., Beijing, China. **YAOBANG ZHAO** is with the Shanghai Spaceflight Precision Machinery Institute, Shanghai, China.